EBSD and Raman Spectroscopy Analysis of Copper Alloy H62/GOp-modified Layer Prepared by Friction Stir Surface Processing

Weiwei SONG [1, 2], Dunwen ZUO [1] *, Yungui SHI [2], Hongfeng WANG [1, 2], Jiafei PU [2]

[1] *College of Mechanical and Electrical Engineering, Nanjing University of Aeronautics and Astronautics, Nanjing, Jiangsu 210016, P. R. China*
[2] *College of Mechanical and Electrical Engineering, Huangshan University, Huangshan, Anhui 245041, P. R. China*

Graphene oxide particles (GOp) were implanted on the surface of H62 copper alloy to prepare an H62/GOp-modified layer by friction stir surface processing (FSSP). The Raman spectrum and microstructure of the modified layer were tested and analyzed. The results showed that the H62/GOp-modified layer prepared under different parameters by FSSP had characteristic Raman spectrum peaks graphene oxide (GO), which indicates that the modified layer containing GO can be prepared by FSSP on the copper alloy surface. The surface grain structure of the H62/GOp-modified layer of each sample was refined, and their large-angle grain boundary ratios were above 85 % and higher than that of the base metal. In addition, the grain volume fraction in the dynamic recrystallization region of each sample was above 60 vol%, and the maximum was 73.9 vol%, which indicates the desirable microstructure consistency of the H62/GOp-modified layer prepared under different parameters by FSSP.
Keywords: microstructure, modified layer, graphene oxide.

1. INTRODUCTION

Copper alloys are widely used in aerospace, high-speed trains, ships, automobiles, and other manufacturing industries due to their good electrical and mechanical properties. However, copper alloy parts are often applied in harsh environments with high humidity, acidity, alkalinity, variable loads, and mutual contact wear. These conditions easily cause the abrasion and corrosion of the copper alloy surface. To improve the wear resistance and corrosion resistance of copper alloys, several scholars use laser cladding, electroplating, thermal spraying, electron beam, ion beam, and chemical vapor deposition to improve the surface properties of copper alloy. Xiang Yonghua et al. [1] used a laser cladding technology to clad titanium to the surface layer of a copper-based alloy to form a wear-resistant second phase to improve the wear resistance of the copper-base alloy surface in a seawater environment. Guo Jialong [2] used the laser cladding technology to select Co, Ni, and Fe-based alloys and mixed them with TaC and TiC-reinforced phases to prepare composite coatings on the copper alloy surface to improve its related properties. Deng Dewei et al. [3] studied the surface layer of Cu-18PB-2Sn copper alloy prepared under different laser powers and observed a large number of holes in its cladding layer. With the gradual increase in laser power, the number of holes in the cladding layer was relatively reduced. Zhou Shengfeng et al. [4] prepared Cu-Fe coating on a copper alloy substrate by laser-induction rapid cladding. The microstructure of the coating consisted of α-Fe and ε-Cu phases and obtained its distribution. Li Yuhai et al. [5] studied previous research results and observed the

imperfect laser surface strengthening of copper alloys and the unclear mechanism. Ke Peng [6] prepared NICR-Cr_3C_2 coating on the surface of copper alloy by supersonic flame spraying technology to improve the surface properties of the alloy. Lv Jike [7] studied the surface modification of annealed T2 red copper and cast HPB59-1 lead brass by using a high-current pulsed electron beam device and analyzed the microstructure and structure of the modified surface. Zhang Li [8] used a metal vapor vacuum arc ion source to inject Zr ions into the copper alloy for surface modification to improve its surface strength and wear resistance. The surface modification of copper alloy studied by the above researchers improved the relevant properties of the copper alloy surface to a certain extent. However, in several key occasions, such as alternating load and large impact environment, the modified layer easily falls off, the modification effect worsens, and the service life of parts is reduced. To improve the surface properties of copper alloys and avoid modified layer shedding, the researchers in this paper studied the effect of friction stir surface processing (FSSP) on the surface of copper alloy in the early stage. FSSP generates friction heat by stirring the surface layer of copper alloy with a tool to recrystallize the surface metal, resulting in grain refinement, to improve the performance of the copper alloy surface. By using FSSP, W, Ni, and Ti powder were implanted on the surface of copper alloy to obtain the corresponding modified surface, and the related properties of the modified surface were improved to a certain extent [9 – 16]. This paper intended to use FSSP to implant graphene oxide particles (GOp) on the surface of H62 copper alloy to prepare an H62/GOp surface layer and analyze the influence of FSSP process parameters on the microstructural change of the prepared surface layer to provide technical support for its subsequent performance analysis.

---

* Corresponding author. Tel.: +86-17768148604.
E-mail address: *imit505@nuaa.edu.cn* (D. Zuo)

2. EXPERIMENTAL MATERIALS AND METHODS

Hot-rolled H62 copper alloy was used in the experiment, and its size was 200×200×10 mm. Table 1 shows the chemical composition of the experimental material.

Table 1. Main chemical composition of H62 Copper alloy (mass fraction, %)

Fe	Pb	Ni	Impurities	Cu	Zn
0.15	0.08	0.5	0.3	60.5-63.5	Balance

Graphene oxide (GO) powder with a purity of more than 96 %, 1 – 2 layers, layer diameter of 0.2 – 10 µm, and a layer thickness of about 1 nm was used in the experiment.

The FSSP experiment adopted the FSW-LM-A10 equipment produced by Beijing FSW Technology Co., LTD., and a needleless tool with a shaft shoulder diameter of 20 mm was used to prepare the modified layer. Fig. 1 shows the FSSP equipment and tool.

Fig. 1. Photograph of friction stir welding equipment and tool
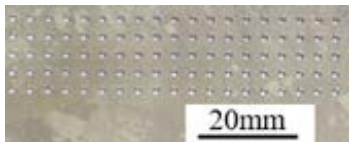
Fig. 2. Photograph of the copper alloy surface drilling

During the preparation of the modified layer, the stirring of the tool was 1 time, the inclination angle was 5°, and the pressure amount was 0.2 mm. Table 2 shows the rotation speed and feed speed of the tool.

Table 2. List of rotation speed and feed speed of the tool

Sample number	The rotating speed of the tool ω, rpm	The feed speed of the tool v, mm/min
1	900	160
2	900	200
3	1100	160
4	1100	200
5	1300	160
6	1300	200

Before the preparation of the H62/GOp-modified layer by FSSP, holes were drilled on the surface of the copper alloy sheet with a hole diameter of 1.5 mm, a hole spacing of 4×3 mm^2, and a depth of 0.3 mm (Fig. 2). Before the modification experiment, the surface layer of the copper alloy was cleaned and dried with water. Then, the surface of the copper alloy plate was cleaned and dried with acetone, water, and anhydrous alcohol successively to ensure that the plate surface was free of oil pollution and other impurities before the experiment. The cleaned copper alloy plate was fixed on the workbench, and a mixed powder (10 % GOp + 90 % Cu) was evenly sprayed on the holes on the copper alloy surface. The mixed powder was compacted to the hole with specialized tools, with paraffin wax sealing the pores, to prevent the modification process stream formed by the tool high-speed from blowing away the powder from the holes. When all the above items were ready, the experiment of H62/GOp-modified layer prepared by FSSP was conducted.

The XploRA Plus laser Raman spectrometer (HORIBA Jobin Yvon, France) was used in the Raman spectrum test. The test wavelength was 532 nm, and the scanning accuracy was ± 0.2 cm^{-1} in the range of 0 – 3500 cm^{-1}. The microstructures were tested and analyzed using Oxford C-Swift EBSD instrument. The sample size was 10×4×4 mm^3. The sample was placed in 30 % HNO$_3$, 70 % methanol, and liquid nitrogen for electrolytic polishing after fine grinding. The current of electrolytic polishing was 1.5 A/cm^2, the voltage was 20 V/cm^2, and the holding time was 20 s.

3. ANALYSIS OF EXPERIMENTAL RESULTS

3.1. Macro morphological analysis

Fig. 3. Photograph of the modified copper alloy surface
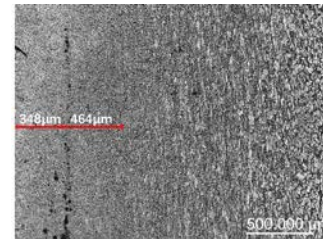
Fig. 4. The metallography of the modified surface profile

Fig. 3 shows the image of the modified surface. The modified surface exhibited fine and uniform arc lines as shown in Fig. 3. This finding shows that the modification process of the tool was consistently in a stable working state. In addition, gray and bronze colors appeared alternately, elucidating the evident effect of modification process of the powder that resulted in a desirable copper alloy plate surface. In the modification process, given the small acting space of the tool, a large amount of friction thermoplasticized mixed powder and substrate surface metal easily gathered during the high-speed rotation and advancement of the tool, which guaranteed the plastic flow of the surface metal. Thus, an excellent modified surface morphology was obtained.

Fig. 4 is a metallographic photograph of the modified surface layer. As can be seen from Fig. 4, the depth of the direct surface modified by FSSP is about 0.35 mm, while the depth of the secondary modified layer affected by FSSP is about 0.45 mm. The thickness of modification is still obvious. In essence, the thickness of the modified layer is mainly the result of the comprehensive effect of FFSP processing parameters, material properties, graphene

particles and other factors, but the pressure of the stirring tool plays a more important role.

3.2. Raman spectroscopy

Fig. 5 shows the characteristic peaks (D, G, and 2G) of GO in each sample under different parameters. The characteristic peak of the GO Raman spectrum of each sample by different parameters was inevident, which is mainly related to the small amount of GO added. Fig. 5 displays the characteristic peak of the GO Raman spectrum, which fully indicates that the modified layer containing GO can be prepared on the copper alloy surface by using FSSP.

3.3. Analysis of microstructure

3.3.1. Grain size analysis

Grain refinement is an effective method to change the comprehensive properties of H62 copper alloy. The yield strength of the alloy increases with the decrease in grain size. In addition, with grain refinement, the total length of grain boundary increases, which has a great influence on the wear resistance and corrosion resistance.

Fig. 6 and Fig. 7 show the orientation image and size distribution of the oriented grains of each sample and base metal, respectively. As shown in Fig. 6 and Fig. 7, the grain size of the modified layer of each sample obtained when the rotating speeds of the tool were 900 and 1100 rpm was in the range of $2-25$ µm, whereas when the rotating speed of the tool was 1300 rpm, the grain sizes of the modified layer were in the range of $1-50$ and $1-60$ µm at the tool feed speeds of 160 and 200 mm/min, respectively. Under all parameters, the grains of the modified layer were refined and showed a uniform distribution. Their grain size ranges were smaller than that of the base metal (the grain size range of the base metal was $0-120$ µm).

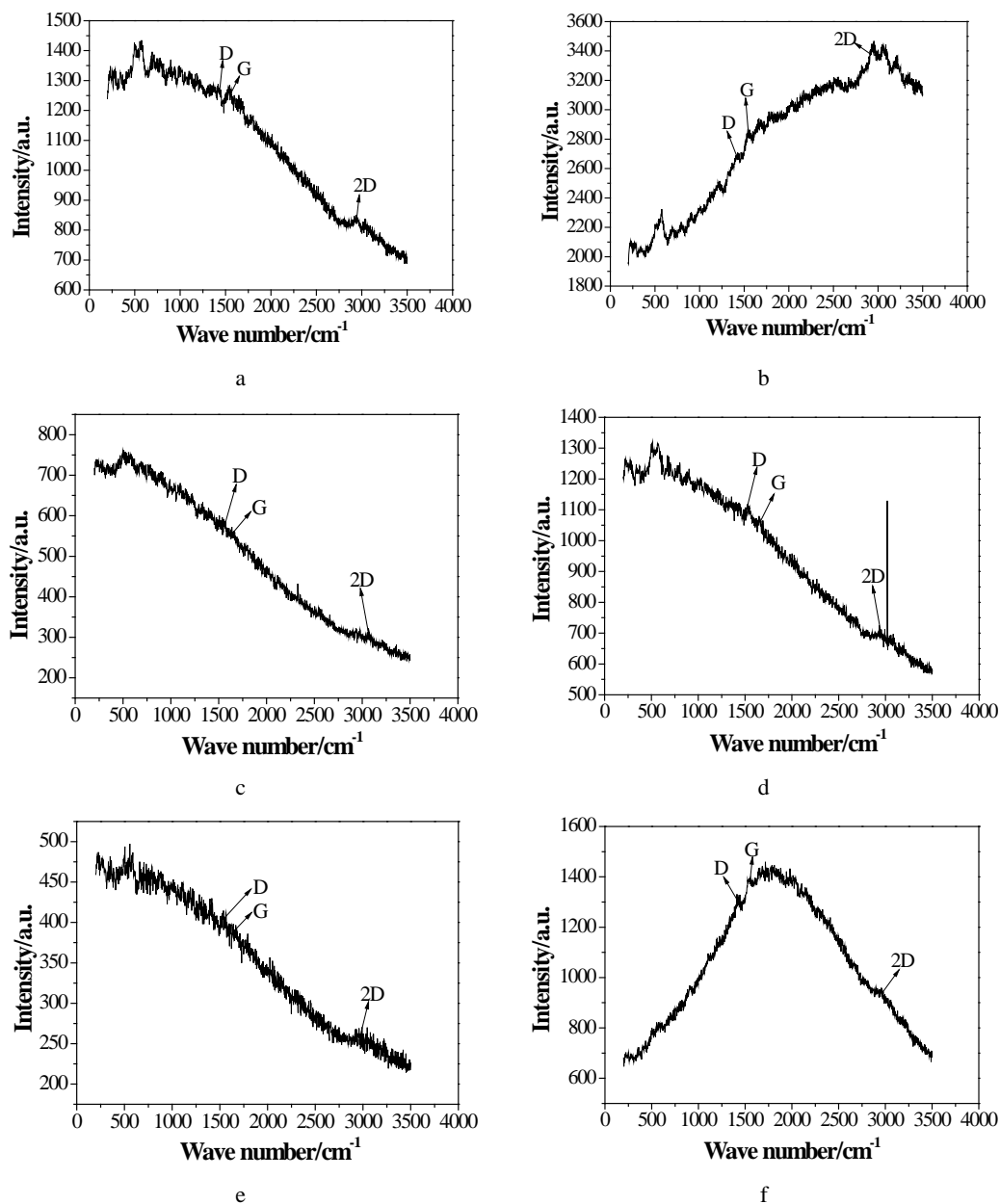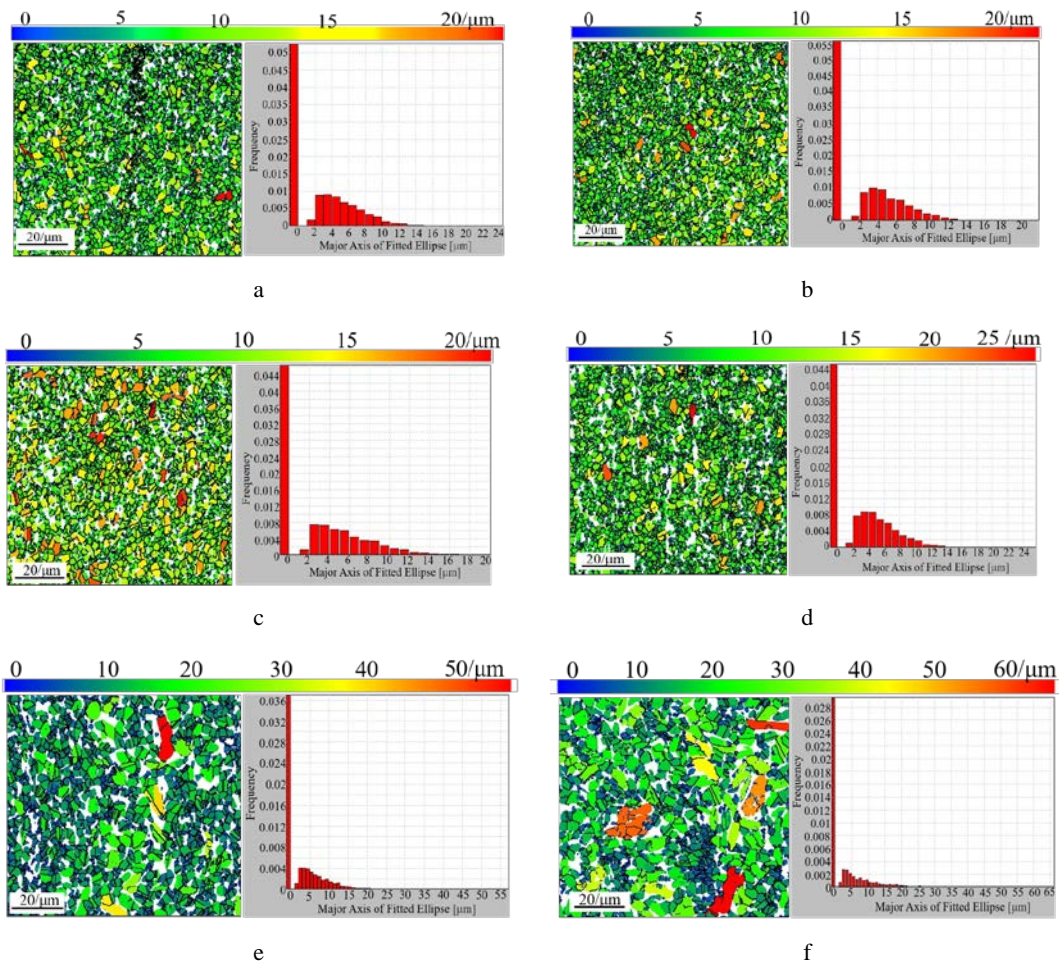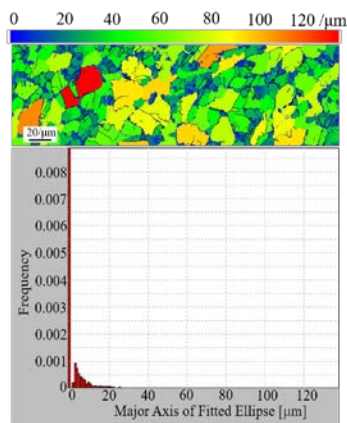**Fig. 5.** Raman spectra of the GO in each sample: a – sample 1; b – sample 2; c – sample 3; d – sample 4; e – sample 5; f – sample 6

Fig. 6. Orientation image and size distribution of the oriented grain of each sample: a – sample 1; b – sample 2; c – sample 3; d – sample 4; e – sample 5; f – sample 6


Fig. 7. Orientation image and size distribution of oriented grain of the base metal

At the constant feed speed of the tool, the grain refinement of the modified layer obtained at the rotation speed of the tool was the most evident, followed by the modified surface layer obtained at the rotation speed of the tool of 1100 rpm. The poorest result was observed with the modified surface layer obtained at the tool rotation speed of 1300 rpm. The grain refinement was due to the large amount of friction heat generated by the high-speed rotation and extrusion advancement of the tool, which resulted in the dynamic recrystallization refinement of the grains of the modified layer. However, when the rotation speed of the tool exceeded a certain range, such as 1300 rpm, high friction stirring heat may be generated. Moreover, given the small space area acted on by the tool, a large amount of heat generated cannot be dispersed within a short time, resulting in the secondary grain growth in the recrystallization process of the modified layer.

3.3.2. Statistics of large- and small-angle grain boundaries

The crystal interface is the interface between grains with the same structure but different orientations. The greater the difference in orientation between different grains, the lower the probability of atoms at the grain boundary being in a coherent state, the more irregular the atomic arrangement, the higher the distortion energy, and the lower the possibility of dislocations crossing the grain boundary. This condition will lead to increased hardness, strength, plasticity, wear resistance, and corrosion resistance at the grain boundary position. Fig. 8 and Fig. 9 show the grain boundary angle statistics of each sample and the base metal, respectively. As it is shown, the large-angle grain boundaries of FSSP modified samples accounted for more than 85 %, and the grain boundary angles were mostly distributed in the range of $20° - 60°$.
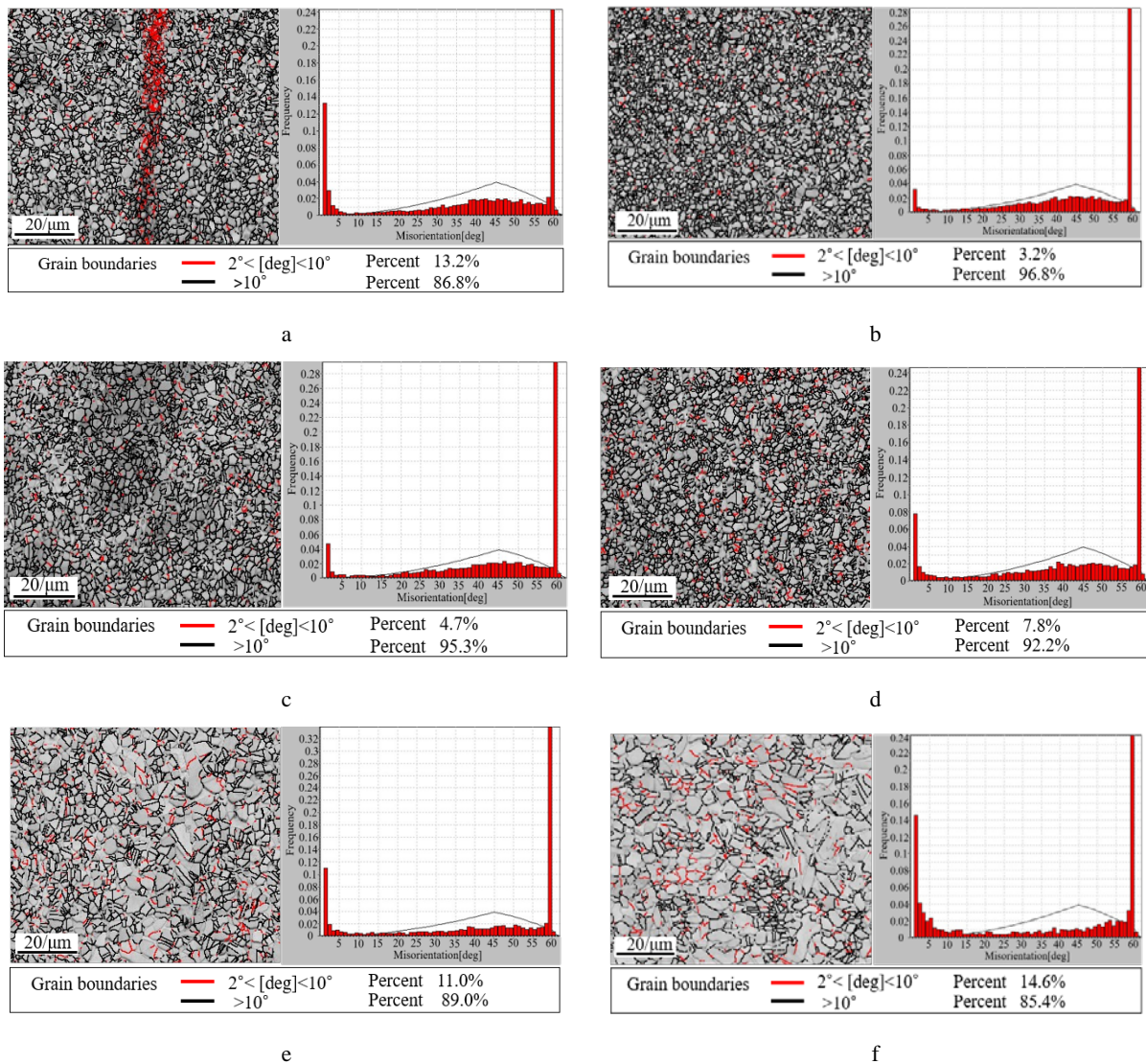
Fig. 8. Grain boundary angle statistics of each sample: a – sample 1; b – sample 2; c – sample 3; d – sample 4; e – sample 5; f – sample 6
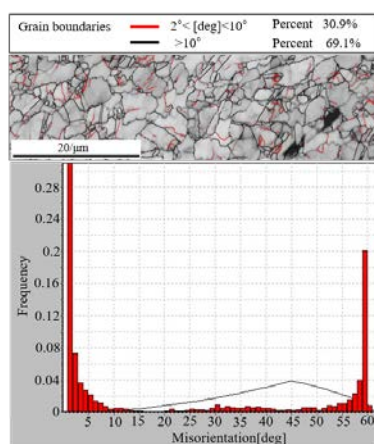

Fig. 9. Grain boundary angle statistics of the base metal

In several samples, the proportion of large-angle grain boundaries was more than 95 %. The ratio of grain boundaries increased with the increase in the angle between grain boundaries, indicating that all grain orientations were distributed, and complete dynamic recrystallization occurred, consistent with the analysis of the overall ingrain orientation. The ratios of large-angle and small-angle grain boundaries of the base metal were about 69.1 % and 30.9 %, respectively. The grain size of all modified samples was smaller than that of the base metal. As shown in Fig. 8 a, small-angle boundaries were concentrated in two strip areas. Fig. 10 a shows that in the deformation zone, the region intracrystalline overall orientation difference was inconsistent, the area exhibited complete dynamic recrystallization caused by local residual stress concentration, the tool edge position was in the process of modification by large centrifugal force and vibration power, and the modification area was caused by large deformation.

Fig. 10 and Fig. 11 show the statistics of in-grain misorientation of each sample and the base metal, respectively. As presented in the figures, the grain volume fraction in the dynamic recrystallization region of the modified area of each sample was above 60 vol%, which is higher than that of the base metal (23.8 vol%). The grain volume fraction in the deformed area was small, and the volume fraction in the least deformed area accounted for 9 vol%. The total proportion of dynamic recrystallization and recovery zones was more than 90 vol%.
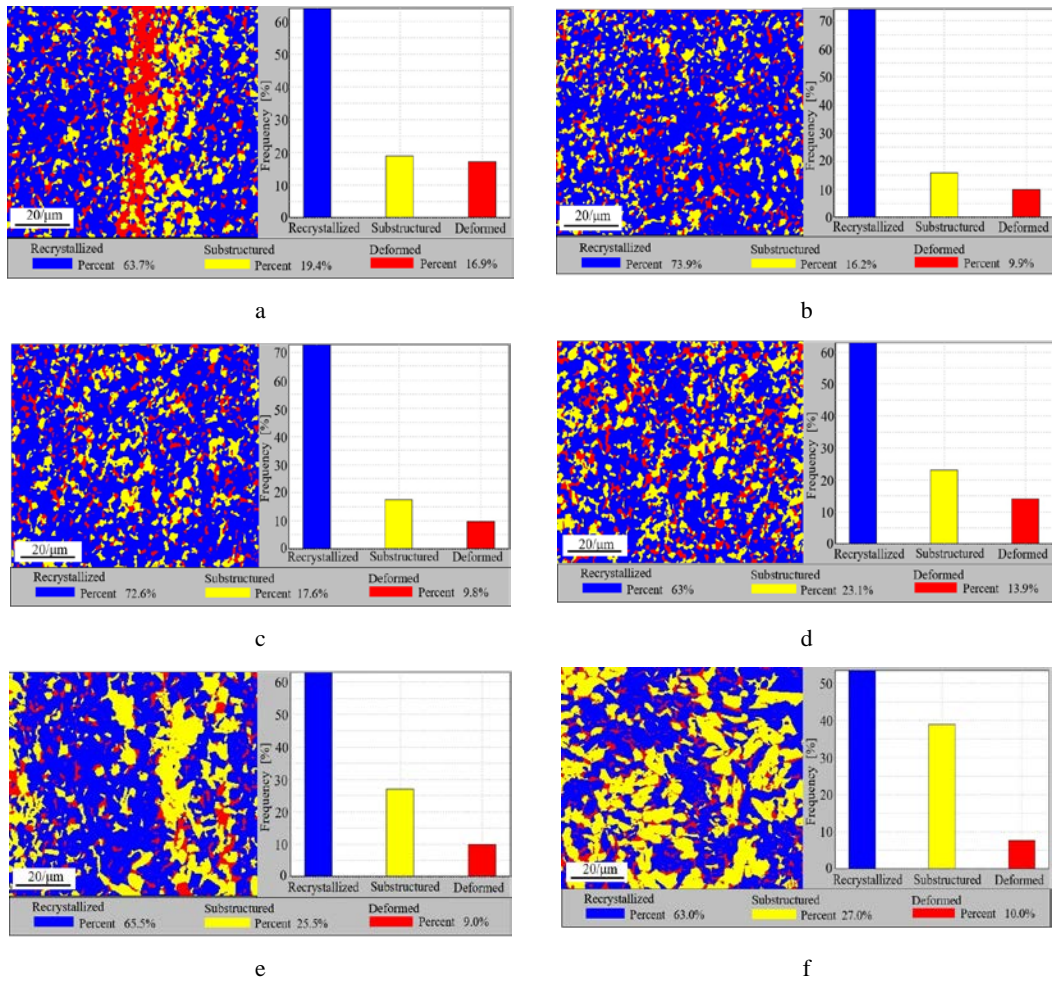
Fig. 10. Statistics of in-grain misorientation of each sample: a – sample 1; b – sample 2; c – sample 3; d – sample 4; e – sample 5; f – sample 6
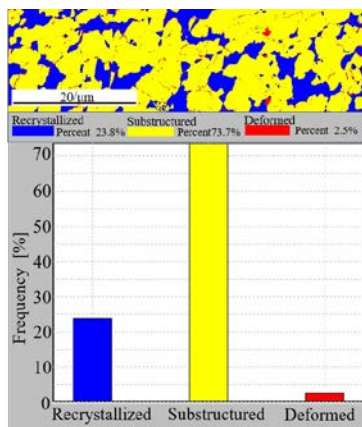
Fig. 11. Statistics of in-grain misorientation of the base metal

3.3.3. Analysis of in-grain global misorientation

This finding was due to the good dynamic recovery and dynamic recrystallization that occurred in this region under the action of friction heat although certain agitation and plastic flow occurred in the FSSP process. Despite the absence of perfect equiaxed grains, several preferred orientations existed, and the uniform consistency of the structure was realized. Thus, FSSP uniformly implanted GOp into the surface layer of the copper alloy.

Fig. 10 also shows that at the constant feed speed of the tool, the grain volume fraction in the dynamic recovery zone of the modified area of the sample increased with the increase in the rotating speed of the tool, which fully indicates that the modified layer metal had good dynamic recrystallization in the modification process. When the tool rotation speed increased to 1300 rpm, the modified process produced substantial friction heat, causing secondary grain growth in the metal modification area. The modified area contained considerable crystal structures and small-angle grain boundaries, large grain size, and crystal grain orientation or low-angle grain boundary position that must be rotated in a reverse direction in response to the organization. The grain sizes are shown in Fig. 6 e and f and the large-angle grain boundary region in Fig. 8 e and f exhibited good correspondence with the recrystallization region in Fig. 10 e and f, that is, secondary grain growth occurred in this region after the input of excessive frictional heat. However, a large proportion of equiaxed grains still existed.

4. CONCLUSIONS

1. The surface of the H62/GOp-modified layer prepared by FSSP was relatively complete, and the resulting arc gap was small, the surface of the stirring area was

32

smooth, and the modified surface showed a good appearance and texture.

2. The surface of the H62/GOp-modified layer prepared under different process parameters of FSSP had the characteristic peak of GO Raman spectrum. Thus, FSSP can be used to prepare modified layers containing GO.

3. According to the analysis of the microstructure of the H62/GOp-modified layer prepared under different process parameters of FSSP, the modified layer possessed a refined grain size, a large-angle grain boundary ratio that was above 85 % and higher than that of the base metal, a grain volume fraction in the dynamic recrystallization region above 60 vol%, and the maximum grain volume fraction of 73.9 vol%. The uniformity of the organization was realized.

REFERENCES

1. **Xiang, Y.H., Chen, Z., Zhao, Y., Xu, F.J., Cui, X.F., Jin, G., Xu, B.S.** Tribological Behaviour of Titanium Modified Copper-based Coating by Laser Cladding in Brine *Surface Technology* 49 (8) 2020: pp. 138 – 144. https://doi.org/10.16490/j.cnki.issn.1001-3660.2020.08.015

2. **Guo, J. L.** Corrosion-resistant Coating on Copper Alloy Surface, Master Thesis, *Shanghai (China): Shanghai University of Engineering Science* 2019. https://doi.org/10.27715/d.cnki.gshgj.2020.000067

3. **Deng, D.W., Zheng, H.T., Ma, Y.S., Chang, Zh.D., Huang, Z.Y.** Study on Microstrctures and Performances of Cu-18Pb-2Sn Coating by Laser Cladding *Journal of Functional Materials* 51 (6) 2020: pp. 06001 – 06006. https://doi.org/10.3969/j.issn.1001-9731.2020.06.001

4. **Zhou, S.F., Zhang, T.Y., Xiong, Z., Dai, X.Q., Wu, Ch., Shao, Zh.Sh.** Investigation of Cu-Fe-based Coating Produced on Copper Alloy Substrate by Laser Induction Hybrid Rapid Cladding *Optics & Laser Technology* 59 2014: pp. 131 – 136. https://doi.org/10.1016/j.optlastec.2013.12.013

5. **Li, Y.H., Wang, Z., Zhao, H., Du, Ch.Y., Wang, J.Ch., Tian, Zh.Y.** Research Progress on Laser Surface Strengthening of Copper Alloy *Journal of Shenyang Ligong University* 38 (6) 2019: pp. 22 – 27. https://doi.org/10.3969/j.issn.1003-1251.2019.06.004

6. **Ke, P.** Preparation and Property Study of NiCr-Cr3C2 Gradient Coating Sprayed by HVOF on Copper Alloy Substrate, Master Thesis, *Anhui (China): Anhui University of Technology* 2017.

7. **Lv, J.K.** Study on Surface Microstructure and Properties of Copper and Copper Alloy after High Current Pulsed Electron Beam Treatment, Master Thesis, *Liaoning (China): Northeastern University* 2014.

8. **Zhang, L.** Surface Modification and Tribological Property of Copper Alloy by Zirconium Ion Implantation, Master Thesis, *Hebei (China): Yanshan University* 2012.

9. **Song, W.W., Xu, X.J., Liu, S.R., Pu J.F., Wang, H.F.** Metallographic Organization and Tensile Properties of FSSP-modified H62 Copper Alloy Surface *Advanced Composites Letters* 29 2020: pp. 1 – 8. https://doi.org/10.1177/2633366X20927025

10. **Song, W.W., Zuo, D.W., Xu, X.J., Wang, H.F., Liu, Sh.R.** Electrochemical Corrosion Performance of FSSP-Modified Copper Alloy Surface *International Journal of Electrochemical Science* 14 (8) 2019: pp. 7026 – 7036. https://doi.org/10.20964/2019.08.23

11. **Song, W.W., Xu, X.J., Liu, S.R., Pu, J.F., Ge, X.L.** Effect on the Wear Resistance of Copper Alloy Surface Modification Layer by FSSP Implanting W Particles *Materials Transactions* 60 (5) 2019: pp.765 – 769. https://doi.org/10.2320/matertrans.m2018316

12. **Song, W.W., Xu, X.J., Zuo, D.W., Wang, J.L., Wang, G.** Effect of Processing Parameters and Temperature on Sliding Wear of H62 Copper Alloy Modified by Friction Stir Surface Processing *Materials Science* 23 (3) 2017: pp. 222 – 226. https://doi.org/10.5755/j01.ms.23.3.16322

13. **Song, W.W., Xu, X.J.** Analysis on Microstructure and Resistance Wear Property of SiC/H62 Copper Alloy the Surface Modified Layer by FSSP *Journal of Functional Materials* 48 (7) 2017: pp. 07205 – 07208. https://doi.org/10.3969/j.issn.1001-9731.2017.07.040

14. **Song, W.W., Guo, H., Wang, H.F.** Analysis of Wear resistance of Copper Alloy Modified Layer by FSSP *Journal of Changzhou Institute of Technology* 32 (2) 2019: pp. 13 – 16+26. https://doi.org/10.3969/j.issn.1671-0436.2019.02.003

15. **Song, W.W., Pan, J., Ge, H., Shen, M., Wang, H.F.** Microstructure Analysis of FSSP Modified H62 Copper Alloy *Journal of Chuzhou University* 21 (2) 2019: pp. 49 – 51. https://doi.org/10.3969/j.issn.1673-1794.2019.02.013

16. **Zhao, S., Wei, Z.B., Fu, X.Y.** Structure and Erosion Wear Resistance of Al -Si -Cu-Fe Die -Casting Alloy Modified by Friction Stir Processing *Materials Protection* 52 (3) 2019: pp. 13 – 17. https://doi.org/10.16577/j.cnki.42-1215/tb.2019.03.003